Determination of the beam asymmetry Σ in η- and η'-photoproduction

JAKOB MICHAEL KRAUSE

Masterarbeit in Physik
angefertigt im Helmholtz-Institut für Strahlen- und
Kernphysik

vorgelegt der
Mathematisch-Naturwissenschaftlichen Fakultät
der
Rheinischen Friedrich-Wilhelms-Universität
Bonn

Sep 2022

I hereby declare that this thesis was formulated by myself and that no sources or tools other than those cited were used.

Bonn, ...
                    Date   Signature

1. Gutachter: Jun. Prof. Dr. Annika Thiel
2. Gutachterin: Prof. Dr. TBD

Acknowledgements

First of all I would like to thank ANNIKA THIEL for giving me the opportunity of being part of her research group since the beginning of my bachelor thesis in 2020. Now, with the formulation of this thesis, I will be finishing my academic career in Bonn. I greatly appreciate the insight into research I could gain.

I express my thanks to REINHARD BECK who agreed to be the second referee for this thesis.

This thesis could not have been written without the help of FARAH AFZAL. After all, it was you, who got me into the boat again after my bachelor thesis. Over the past year we have shared our office and many fruitful discussions regarding physics (or not) were had. I am thankful that you and your masters and PhD thesis provided such excellent foundation for me to rely my work on.

Being the pioneer of the working group BECK/THIEL in all things regarding BAYESIAN statistics, PHILIPP KRÖNERT contributed the idea of what shall fill about half of this thesis and furthermore his help and guidance whenever i got stuck on the way. I am grateful that we were able to turn the thesis into this direction with your help.

Also, I express my gratitude to everybody who was included in the process of data taking, i.e. the CBELSA/TAPS collaboration and crew. No analysis could have been performed without the data.

I thank FARAH AFZAL, PHILIPP KRÖNERT, DOMINIC SCHÜCHTER and NIKOLAS PÄSSLER for reading my thesis and providing me with useful comments and insights.

Finally, I thank my parents, for the (financial) support throughout my whole studies, which now then officially come to an end.

Contents

Introduction

The *Standard Model of Particle Physics* (SM) is the most successful model aiming to describe the particles and forces of the universe. It distinguishes between *fermions* and *bosons*. While all matter consists of fermions, bosons are particles that mediate the fundamental interactions.

Matter consists of (anti-)quarks and (anti-)leptons with three generations of each. Table 1.1 shows all elementary fermions including some of their most important properties. Only the first and lightest generation consists of stable particles, i.e. the up and down quark as well as the electron and its neutrino. All other particles are heavier and not stable, they will thus decay fast via the strong, electromagnetic or weak interaction.

There are in fact four interactions described by the SM: strong, electromagnetic, weak and gravitational interaction [1], where gravitation is mentioned here for the sake of completeness; on the mass scale of elementary particles gravitation is negligible. Strong and weak interaction are restricted to a finite range of the order of the nucleon radius, whereas electromagnetic interaction and gravitation have infinite range. Each interaction has its own coupling (charge). The strong interaction is mediated by gluons and couples to the color charge.

	Generation			el. charge	color charge
	1	2	3		
Quarks	u	c	t	2/3	r,g,b
	d	s	b	1/3	r,g,b
Leptons	e	μ	τ	-1	-
	ν_e	ν_μ	ν_τ	0	-

Table 1.1: Summary of the particles of the SM

Gluons and quarks carry color charge and thus interact strongly. However, an isolated quark or gluon has not been observed. Only color neutral bound systems of quarks are seen, which are called hadrons. Hadrons with integer spin are called mesons and those with half-integer spin are called baryons. Color neutrality demands mesons consist of at least one quark and one anti-quark and baryons consist of at least three quarks.

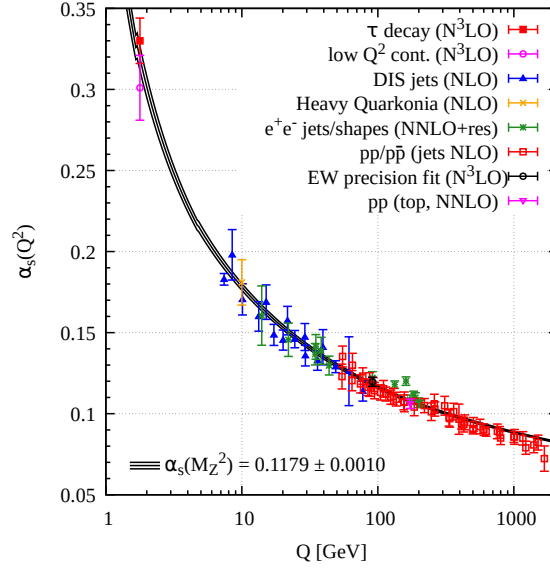[1] they are ordered here according to their relative strength

Figure 1.1: Running coupling of QCD. The colored data points represent different methods to obtain a value for α_s. For more details it may be referred to [Zyl+20].

As already mentioned, isolated quarks are not seen. This can be understood in terms of the strong coupling constant α_s. The coupling constant is a measure of the strength of the strong interaction. Because it is highly dependent on the momentum transfer in the observed strong reaction it is also called running coupling constant, which is depicted in figure 1.1.

For low (< 1 GeV) momentum transfers or large distances the coupling constant approaches infinity whereas it decreases for high ($\gg 1$ GeV) momentum transfers or short distances. These momentum ranges are referred to as *confinement* and *asymptotic freedom*, respectively; quarks are confined to remain in a bound state since if one tried to pull them apart the color field becomes so strong it will create a new quark anti-quark pair resulting in two new bound states. On the other hand, bound quarks behave quasi-free and can be described using perturbative quantum chromodynamics (pQCD) if probed at sufficiently large momentum transfers.

It is more difficult however to describe QCD at momentum scales of ≈ 1 GeV since the coupling is too strong to justify a perturbative approach. Thus explicit modeling of QCD bound states is inevitable. One possibility is to describe baryons consisting of constituent quarks which are bound in a potential. Constituent quark models assume baryons are made up of three constituent quarks with effective masses differing from the bare quark mass. The effective mass is made up mostly from a sea of quark anti-quark pairs and gluons which surround the bare (valence) quarks. The explicit form of the binding potential is determined for each model.

The Bonn model [LMP01], for example, is formulated as a relativistically covariant constituent quark model. A potential increasing linearly with the distance is employed to adequately describe confinement. The binding potential between the constituent quarks is described by an instanton-induced interaction. Baryon resonances are then states with an orbital or angular excitation of one of the quarks. Figure 1.2 shows computed nucleon, that is Isospin $I = 1/2$ resonances, of the Bonn model [LMP01] on the left side of each column. These are compared to measured resonances and their PDG rating [Zyl+20] in the middle. Uncertainties are indicated by the colored areas. The resonances are

identified by their total angular momentum and their parity $J\pi$. In addition also the total internal angular momentum along with isospin and again the total angular momentum L_{2T2J} is given. While
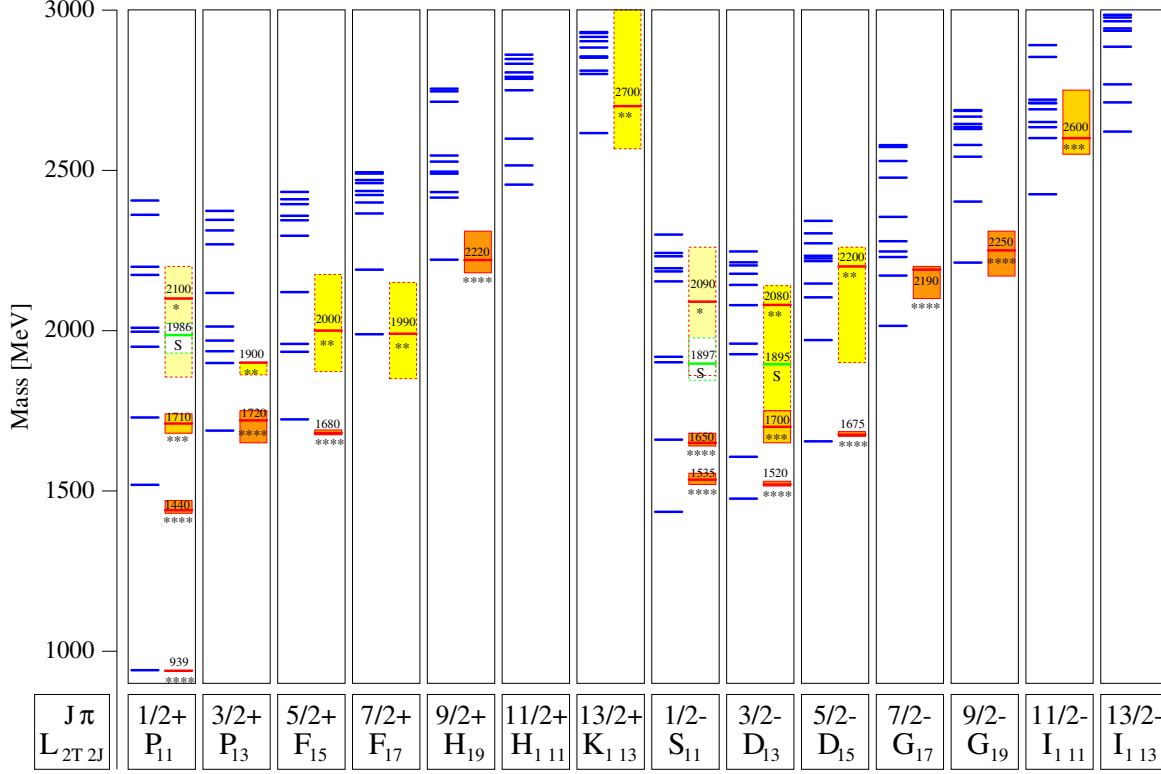

Figure 1.2: Calculated nucleon (isospin $I = 1/2$) resonances compared to measurements. Left in each column are the calculations [LMP01], the middle shows the measurements and PDG rating [Zyl+20]

generally good agreement exists for low lying resonances, especially for high masses there are much more resonances predicted than actually found. This is also known as the problem of the "missing resonances" indicating the poor understanding of QCD in the non-perturbative region. This can be due to several reasons: most of the knowledge about nucleon resonances and their properties was obtained investigating the πN channel, biasing the data for resonances coupling weakly to this channel. Furthermore, the number of excited states with definite quantum numbers is related directly to the effective number of degrees-of-freedom accessible to the underlying theory. As a consequence, the number of degrees-of-freedom should be obtainable by comparing the measured states to the predicted states. Since nucleon resonances decay dominantly hadronic, their resonances are broad and overlapping. Thus on one hand the determination of excitation spectra proves to be a challenge on its own, demanding sophisticated methods, such as partial wave analysis (PWA). On the other hand it is not yet clear how many effective degrees-of-freedom exist for the nucleon in a constituent quark model. They could for example be decreased if the nucleon were made up of a quark and a di-quark structure. In either case it should prove fruitful to investigate the photoproduction of mesons off the nucleon for different final states to access the resonances and transitions between them which are of interest. This should ultimately add to the understanding of QCD in the non-perturbative regime. [KS03]

1.1 Photoproduction of Pseudoscalar Mesons

From the scattering theory point of view, photoproduction of mesons is well understood [KS03]. Figure 1.3 shows schematically the process thereof off the proton:
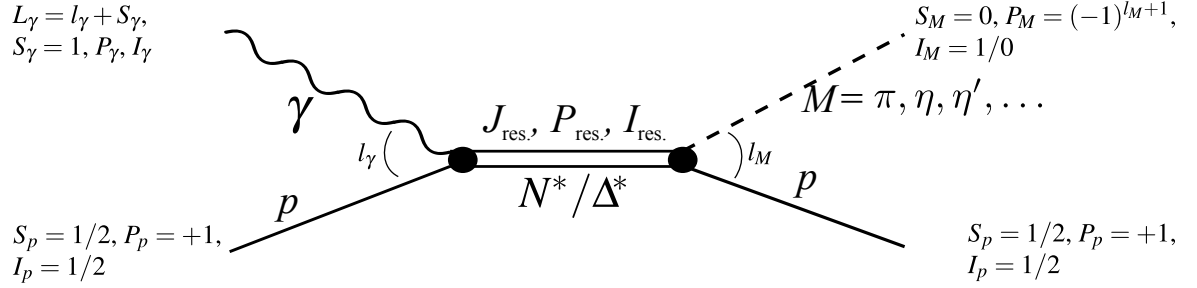

$L_\gamma = l_\gamma + S_\gamma,$
$S_\gamma = 1, P_\gamma, I_\gamma$

$S_M = 0, P_M = (-1)^{l_M+1},$
$I_M = 1/0$

γ

$J_{\text{res.}}, P_{\text{res.}}, I_{\text{res.}}$

$M = \pi, \eta, \eta', \dots$

l_γ

l_M

N^*/Δ^*

p

p

$S_p = 1/2, P_p = +1,$
$I_p = 1/2$

$S_p = 1/2, P_p = +1,$
$I_p = 1/2$

Figure 1.3: FEYNMAN diagram for the s-channel photoproduction of pseudoscalar mesons, adapted from [Afz19]

The analysis requires partial wave decomposition in both initial and final states [DT92] since the intermediate resonance has definite angular momentum, parity and isospin $J_{\text{res.}}, P_{\text{res.}}, I_{\text{res.}}$. The resonance is excited by a photon with (iso-) spin $I_\gamma, S_\gamma = 1$ and parity P_γ coupling electromagnetically to the target proton with (iso-) spin $I_p = 1/2, S_p = 1/2$ and parity P_p. The relative momentum is l_γ, such that the total momentum of the photon is $L_\gamma = l_\gamma + S_\gamma$. Subsequently the intermediate state will have the quantum numbers $J_{\text{res.}}, P_{\text{res.}}, I_{\text{res.}}$ and decay into a pseudoscalar ($S_M = 0$) meson with isospin I_M, relative orbital angular momentum l_M und Parity $P_M = (-1)^{l_M+1}$ and a proton. The following selection rules can be derived using parity and momentum conservation [KS03; Afz19]

$$J_{\text{res.}} = L_\gamma \oplus S_p = L_\gamma \oplus 1/2, \tag{1.1}$$

$$P_{\text{res.}} = P_p \cdot P_\gamma = P_\gamma, \tag{1.2}$$

$$J_{\text{res.}} = l_M \oplus S_p = l_M \oplus 1/2 \tag{1.3}$$

$$P_{\text{res.}} = P_p \cdot P_M = (-1)^{l_M+1}, \tag{1.4}$$

where the usual rules for the coupling of angular momenta [Bar+18] apply. Thus, knowledge of the photoproduction multipoles allows the identification of contributing resonances for particular mesonic final states. Table 1.2 shows relevant resonances for the lowest order of photon multipoles ($L_\gamma = 1$).

E

Table 1.2: Allowed quantum numbers for the intermediate resonance state N^*/Δ^*

1.2 Measurement of Polarization Observables

1.3 Introduction to Bayesian statistics

1.3.1

1.4 Motivation and Structure of this Thesis

bla

Experimental Setup

As motivated in the previous chapter, it is promising to study the photoproduction of pseudoscalar mesons in order to determine a complete set of polarization observables. This requires a polarized photon beam and/or a polarized target. It is convenient to study photoproduction off a fixed target and investigate the resonances that occur in the process. Incidentally, these resonances can only be accessed via their decay products, such that suitable calorimeters are needed. The CBELSA/TAPS experiment is located in Bonn at the ELectron Stretcher Accelerator (ELSA), which can be used to generate a high energy photon beam using the *bremsstrahlung* process, meets all above mentioned requirements. This chapter will elaborate on the already mentioned parts of the experiment that was used to collect the data needed for the determination of the target asymmetry in η' photoproduction.

2.1 Production of (polarized) high energy photon beam

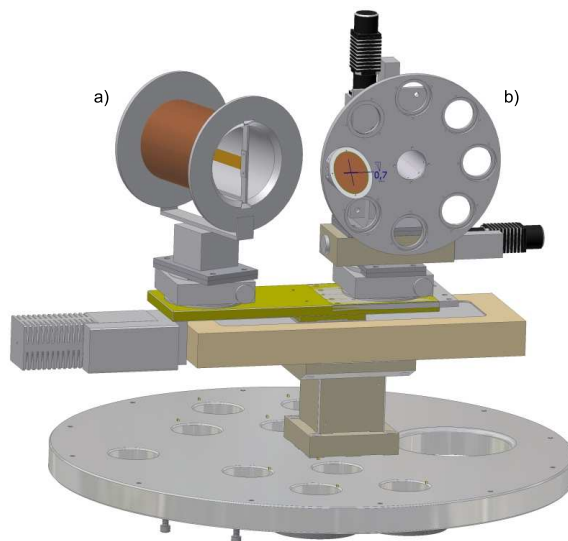First of all, a high energy photon beam has to be produced.
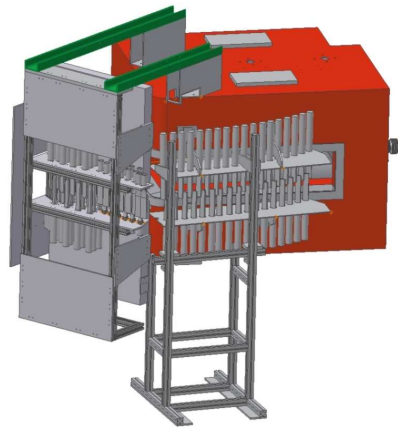

Figure 2.1: [Wal]

Figure 2.2: [Wal]

2.1.1 Tagger

2.2 Beam Target

Figure 2.3: [Wal]

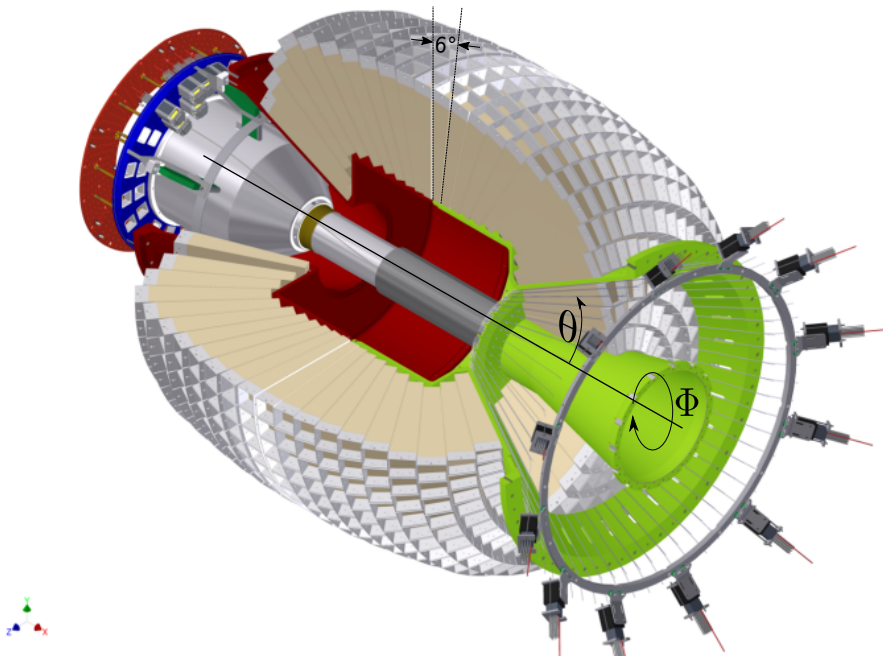## 2.3 Calorimeters

2.4 Trigger

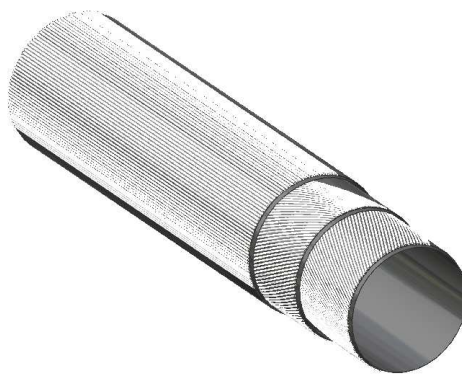**Figure 2.4:** D. WALTHER in [Urb17]
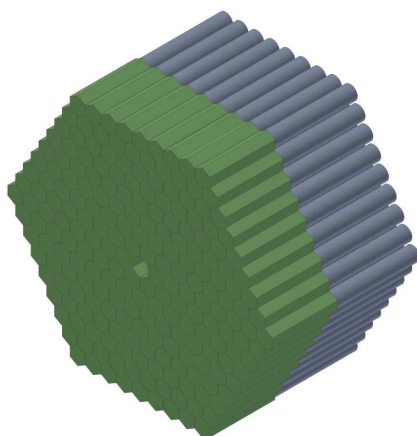

Figure 2.5: [Wal]

Figure 2.6: [Wal]

Event selection

The determination of polarization observables needs to be completed for particular reactions (cf. chapter 1), such as the photoproduction of e.g. a single η' meson. However, the recorded events contain data from the decay products of all possible final states in addition to combinatorical background. Thus, event candidates for the desired reaction have to be extracted before they are considered for further analysis. Table 3.1 shows the five most probable decay modes of the η' meson. Three of these result in final states which only contain photons and are thus accessible for reliable measuring with the CBELSA/TAPS experiment. Only the $\eta' \rightarrow \gamma\gamma$ decay channel was considered for further analysis; the $\omega\gamma$ channel provides negligible statistics and considering the acceptance of detecting six photons in the final state, the expected yield of the $\eta' \rightarrow \gamma\gamma$ decays should be roughly equal to the $\eta' \rightarrow \pi^0\pi^0\eta \rightarrow 6\gamma$ final state [Afz22]. Offering a cleaner, three-particle final state, the $\eta' \rightarrow \gamma\gamma$ was then favored in the course of this thesis. The process of *event selection* for the reaction $\gamma p \rightarrow p\eta' \rightarrow p\gamma\gamma$ is outlined in

Decay mode		Branching ratio
$\pi^+\pi^-\eta$		42.6%
$\rho^0\gamma$	$\rightarrow \pi^+\pi^-\gamma$	28.9% (28.9%)
$\pi^0\pi^0\eta$	$\rightarrow 6\gamma$	22.8% (8.8%)
$\omega\gamma$	$\rightarrow (\pi^+\pi^-\pi^0\gamma/\pi^0\gamma\gamma)$	2.52% (2.2%/0.21%)
$\gamma\gamma$		2.3%

Table 3.1: The five most probable decay modes of the η' meson. The most probable further decay with according branching ratio is shown in brackets.[Zyl+20]

the following chapter.

3.1 Charge cut

3.2 Time of particles

Due to its high count rate the tagging system (see section 2.1.1) will not only record beam photons which produce the detectable final state particles, but also several uncorrelated beam photons. To select only beam photons which will induce a photoproduction process the time information of the

detected particles is used. It is shown in figure 3.1 for all particles involved in 3PED events of η' photoproduction. In all cases prompt peaks centered around 0 ns (the trigger time) are visible. Since the final state photons move with velocity c their timing information does not underlie fluctuations, as is the case for the final state proton on the contrary. The tagged, uncorrelated beam photons are visible as flat background underneath the prompt peak in the time of the beam photon.
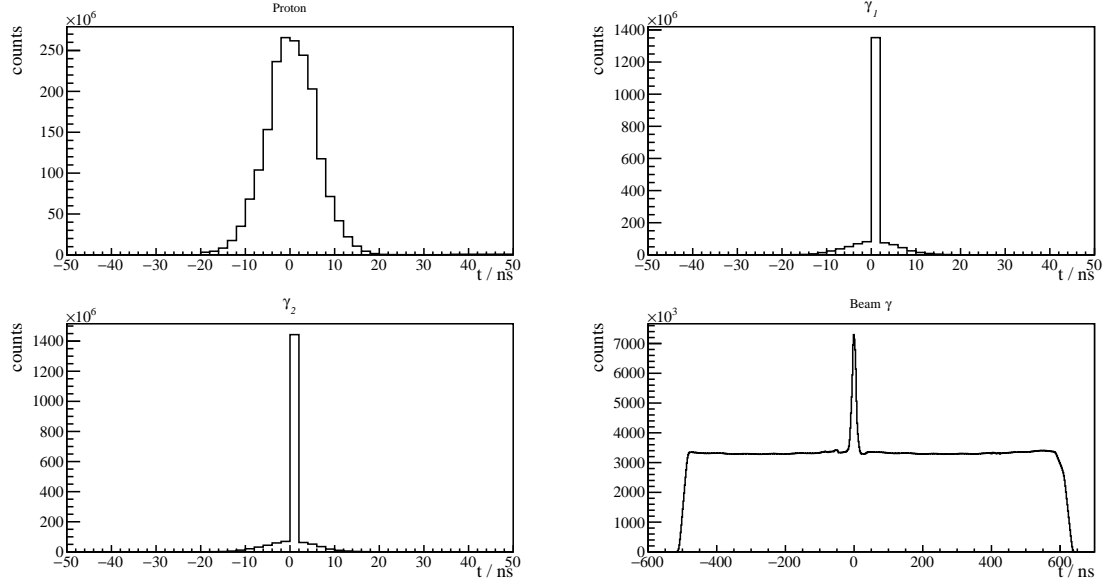

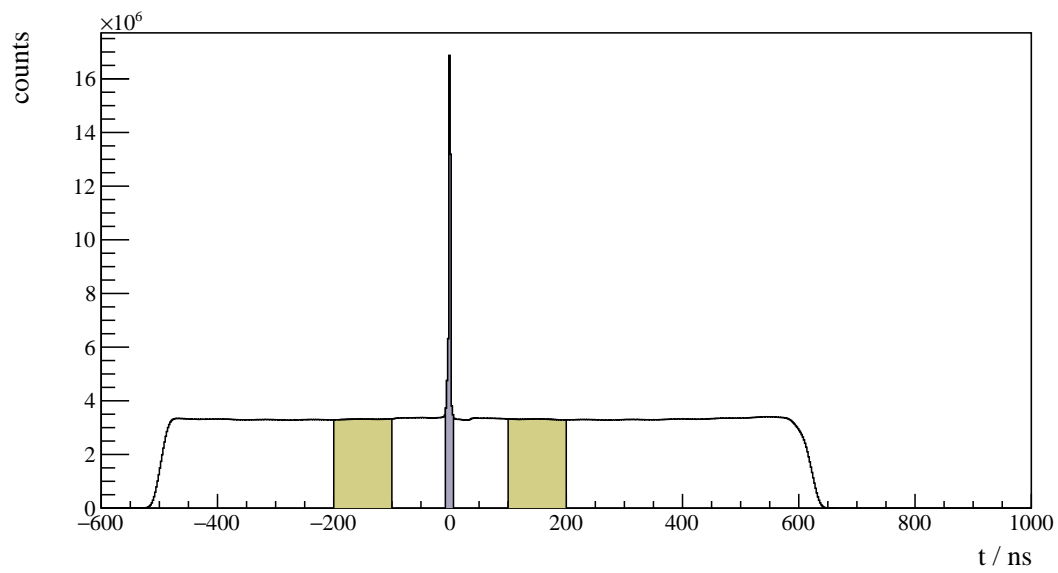**Figure 3.1:** Time information of all final state particles and the beam photon for 3PED η' production

Figure 3.2: Reaction time t_r for 3PED η' production

Determination of the beam asymmetry Σ_η

4.1 Bayesian fit to event yield asymmetries

4.1.1 Application of method to toy Monte Carlo data

4.1.2 Application of method to real data

4.2 Event based fit

4.2.1 Application of method to toy Monte Carlo data

4.2.2 Application of method to real data

4.3 Discussion

Determination of the beam asymmetry $\Sigma_{\eta'}$

5.1 Fit to event yield asymmetries

5.1.1 Application of method to toy Monte Carlo data

5.1.2 Application of method to real data

5.2 Event based fit

5.2.1 Application of method to toy Monte Carlo data

5.2.2 Application of method to real data

5.3 Discussion

Summary and outlook

Useful information

In the appendix you usually include extra information that should be documented in your thesis, but not interrupt the flow.

The LaTeX WikiBook [**latexwiki**] is a useful source of information on LaTeX.

Bibliography

[Zyl+20]   P. Zyla et al., *Review of Particle Physics*, PTEP **2020** (2020) 083C01 (cit. on pp. 2, 3, 11).

[LMP01]   U. Löring, B. Metsch and H. Petry, *The light-baryon spectrum in a relativistic quark model with instanton-induced quark forces*,
The European Physical Journal A **10** (2001) 395, ISSN: 1434-601X,
URL: http://dx.doi.org/10.1007/s100500170105 (cit. on pp. 2, 3).

[KS03]   B. Krusche and S. Schadmand,
Study of nonstrange baryon resonances with meson photoproduction,
Prog. Part. Nucl. Phys. **51** (2003) 399, arXiv: nucl-ex/0306023 (cit. on pp. 3, 4).

[Afz19]   F. N. Afzal, *Measurement of the beam and helicity asymmetries in the reactions*
$\gamma p \rightarrow p\pi^0$ *and* $\gamma p \rightarrow p\eta$,
PhD thesis: Rheinische Friedrich-Wilhelms-Universität Bonn, 2019,
URL: https://hdl.handle.net/20.500.11811/8064 (cit. on p. 4).

[DT92]   D. Drechsel and L. Tiator, *Threshold pion photoproduction on nucleons*,
J. Phys. G **18** (1992) 449 (cit. on p. 4).

[Bar+18]   M. Bartelmann et al., *Theoretische Physik 3 — Quantenmechanik*, 2018,
ISBN: 978-3-662-56071-6 (cit. on p. 4).

[Wal]   D. Walther, *Crystal Barrel, A 4π photon spectrometer*,
URL: https://www.cb.uni-bonn.de (visited on 27/09/2021) (cit. on pp. 7–10).

[Urb17]   M. Urban, *Design eines neuen Lichtpulsersystems sowie Aufbau und Inbetriebnahme der neuen APD Auslese für das Crystal-Barrel-Kalorimeter*,
PhD thesis: Rheinische Friedrich-Wilhelms-Universität Bonn, 2017 (cit. on p. 9).

[Afz22]   F. Afzal, *Private communication*, 2022 (cit. on p. 11).

List of Figures

List of Tables